Volume 16 Number 8 1988 Nucleic Acids Research

The TFIIIA recognition fragment d(GGATGGGAG)·d(CTCCCATCC) is B-form in solution

Fareed Aboul-ela, Gabriele Varani, G.Terrance Walker and Ignacio Tinoco, Jr

Department of Chemistry and Laboratory of Chemical Biodynamics, University of California, Berkeley, CA 94720, USA

Received December 2, 1987; Revised and Accepted March 16, 1988

ABSTRACT

The deoxyoligonucleotide d(GGATGGGAG)·d(CTCCCATCC) is a portion of the gene recognition sequence of transcription factor IIIA (TFIIIA). The crystal structure of this oligonucleotide was shown to be A-form (Mc Call, M., Brown, T., Hunter, W. N., and Kennard, O. 1986 Nature **322**, 661-664). The present study employs NMR, optical, chemical and enzymatic techniques to investigate the solution structure of this DNA 9-mer. NMR COSY experiments indicate 16 of the 18 residues are predominantly south (C_2'-endo) sugar conformation. NMR NOESY indicates glycosidic angles in the range predicted for B-form DNA as opposed to A-form. Related DNA and RNA self-complementary 18-mer sequences, d(GGATGGGAGC-TCCCATCC), with U substituted for T in RNA, were studied by circular dichroism. CD spectra support B-form structures for the DNA 9-mer and the DNA 18-mer, and A-form for the RNA 18-mer. High trifluoroethanol concentrations induce a B- to A-form transition in the DNA oligonucleotides. Enzymatic and chemical probes also illustrate significant differences between the DNA and the RNA oligonucleotides. We find no evidence to support an A-form conformation for the TFIIIA recognition sequence d(GGATGGGAG)·d(CTCCCATCC) in solution.

INTRODUCTION

Transcription factor III A (TFIIIA) from Xenopus Laevis binds to an internal region of the gene for 5S ribosomal RNA and participates in activation of the gene (1). Nuclease digestion and methylation protection experiments suggested that the gene binding site of TFIIIA exhibited A-form conformational features (2, 3). These enzymatic mapping experiments, in conjunction with the ability of the protein to bind both the control region of the gene and the 5S RNA (4) led Klug and coworkers to propose that TFIIIA recognizes an A-form geometry (3).

Further support for an A-form TFIIIA binding site was provided by an A form crystal structure (5) for the deoxyoligonucleotide d(GGATGGGAG)·d(CTCCCATCC) which represents the strongest binding site (3, 6) of the gene (base pairs 81 to 89 of the gene). Similar findings of A-form crystal structure have been reported for other G·C rich DNA sequences (7, 8). However, nuclear magnetic resonance (NMR) and optical spectroscopy techniques (circular dichroism, Raman) have demonstrated that the conformation of a specific deoxyoligonucleotide can significantly differ in solution and crystal (9, 10). Indeed, recent circular dichroism (CD) studies have contradicted the proposal of A-form geometry for the 54 base pair 5S RNA gene sequence recognized by TFIIIA (11). Therefore, solution studies of the same deoxyoligonucleotide crystallized

by Kennard and coworkers appear to be necessary to fully characterize the structure of this portion of TFIIIA recognition sequence.

NMR has been used succesfully to discriminate between different nucleic acid conformations in solution (12, 13). In particular, two-dimensional correlated spectroscopy (COSY) experiments are sensitive to the geometry of the sugar residue, while 2D-nuclear Overhauser enhancement (NOESY) experiments are sensitive to interproton distances. Distances derived from NOESY data can be compared with distances from X-ray crystallography for different DNA conformations. We have investigated the solution structure of the DNA oligonucleotide d(GGATGGGAG)·d(CTCC-CATCC) using these NMR techniques and circular dichroism (CD), which is sensitive to the stacking of the bases (14).

In order to explore the basis of TFIIIA binding to both DNA and RNA , and specifically the possibility that TFIIIA is recognizing a common structure in both DNA and RNA, comparison of the structural properties of the DNA 9-mer with an RNA oligomer of identical sequence was deemed advantageous. However, since it is easier to synthesize longer RNA oligomers using T7 RNA polymerase (15), we chose to synthesize a self-complementary 18-mer consisting of the two above strands in succession. DNA and RNA 18-mers GGATGGGAGCTCCCATCC (with U substituted for T in RNA) were synthesized and compared using circular dichroism, and chemical and enzymatic digestions. The structure of this TFIIIA recognition fragment has also been tested by examining the CD of the deoxyoligonucleotide at high trifluoroethanol (TFE) concentrations, since TFE is known to induce a B to A transition in DNA.

MATERIALS AND METHODS

Oligonucleotide synthesis and purification

DNA oligonucleotides were synthesized on an Applied Biosystems 381A instrument. The RNA oligonucleotide was synthesized using T7 RNA polymerase and an oligomeric DNA template (15). Purification of the two DNA 9-mer strands was by reverse phase HPLC and desalting on a G10 column (Pharmacia) followed by extensive dialysis. The DNA and RNA 18-mers were purified by preparative 20% acrylamide gel electrophoresis under denaturing conditions (7M urea). The purity of the samples was checked by 20% acrylamide gel electrophoresis. Terminal 5' triphosphates, which are a product of synthesis by T7 RNA polymerase, were removed with calf intestinal phosphatase (Boehringer-Mannheim) followed by purification on Sep-pak cartridges (Millipore).

Circular Dichroism (CD)

CD spectra were recorded on a Jasco J500C spectropolarimeter at 25 °C using 1 cm path-length cuvettes. Nucleotide concentrations were 50 μM. Values of $\Delta\varepsilon$ are expressed in terms of nucleotides.

Chemical digestion

Copper phenanthroline digestion studies with ^{32}P labeled oligonucleotides were at room

temperature following the procedure of Ref 16. Digestion mixtures were quenched as a function of time with 7mM EDTA, 4 M urea (final concentrations). Each aliquot was run on a 20% acrylamide, 7M urea denaturing gel. Full length oligonucleotide bands were cut and the amount of radioactivity counted on a liquid scintillation counter.

NMR

NMR samples were lyophilized several times with 99.8% D_2O and then diluted to ~2 mM in strands with 0.4 ml of 10 mM sodium phosphate, 50 mM NaCl, 0.1 mM Na_2EDTA (pH 7) in 99.96% D_2O(Aldrich). 2D-NMR spectra were recorded at 500 Mhz on a General Electric GN-500 spectrometer at 30°C, well below the melting temperature of the double strand ($T_m \approx 50$ °C under the present conditions). Linewidths were somewhat broadened at lower temperatures, whereas signs of premelting were apparent in 1D-NMR spectra above 35 °C. Phase sensitive NOESY spectra at different mixing times were recorded using the TPPI method (17); the mixing times were 60, 120, 200 and 250 ms; the sweep width 4032 hz. 450 FID's were collected and 2K complex data points recorded for every FID. Data were zero filled to 1K real points in t_1, and apodized prior to fourier transformation using a skewed sine bell (phase shift 60°, skewedness 0.7) in both dimensions. Deviations from linearity in the cross peak intensities as a function of mixing time were observed in buildup rates for NOEs, but the qualitative trends described here were evident at all mixing times. The phase sensitive COSY spectrum was recorded using the TPPI technique (17) with presaturation of the HDO peak. 750 FID's, each of 8K complex data points were collected; the sweep width was 4000 hz. High digital resolution (1 hz) was desirable though not necessary to measure the coupling parameters. Data were zero filled to 4K real points in t_1 and a 30° phase shifted skewed sine-bell (skewedness 0.7) was used for apodization in t_1 and t_2.

RESULTS

CD

Circular dichroism is sensitive to stacking interactions and large differences exist between the CD spectra of A- and B-form nucleic acids (14, 18-20). Hallmarks of A-form RNA and A-form DNA are CD spectra with large positive magnitude at 270 nm, slight negative magnitude at 240 nm and large negative magnitude at 210 nm. In contrast, B-DNA of identical sequence generally exhibits a conservative CD spectrum with less positive magnitude around 270 nm, greater negative magnitude at 240 nm and near zero magnitude at 260 and 210 nm (19, 20). CD spectra for the DNA 18-mer d(GGATGGGAGCTCCCATCC)$_2$ and the RNA 18-mer r(GGAUGGGAGCUCCCAUCC)$_2$ are shown in Fig. 1a. Comparison of the RNA and DNA spectra clearly support a DNA conformation distinct from the RNA conformation. The CD spectrum of the DNA 9-mer is also consistent with a B-form conformation (data not shown). The DNA spectra are qualitatively similar to that reported for a 54 base pair fragment corresponding to the full TFIIIA binding site (11), suggesting that the B-form structure observed here is not an artifact due to end effects. CD

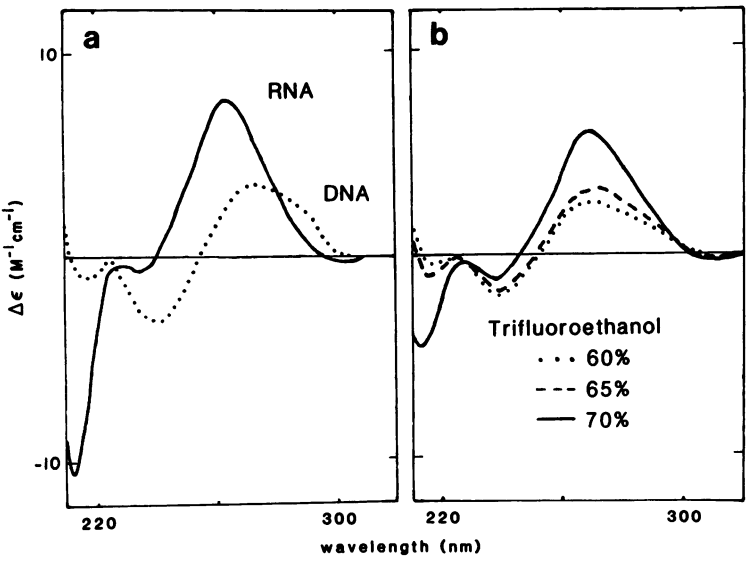

Figure 1

(a) CD spectra for the DNA 18-mer (·····) d(GGATGGGAGCTCCCATCC) and the RNA 18-mer (——) r(GGAUGGGAGCUCCCAUCC) in 50 mM NaCl, 8mM Na_2HPO_4, 0.1 mM Na_2EDTA, pH 7, 25 °C.

(b) B to A transition in the DNA 18-mer induced by trifluoroethanol (TFE). CD spectra for the DNA 18-mer in 2mM NaCl, 0.1 mM Na_2EDTA, 25 °C at the indicated TFE concentrations (v/v).

spectra were calculated for these oligonucleotides according to the method of Gray and coworkers (19, 20) which uses an empirical basis set of DNA and RNA polynucleotide spectra . Observed and calculated spectra qualitatively agree, and support respective B- and A-form conformations for the DNA and RNA oligonucleotides.

CD studies have shown that trifluoroethanol (TFE) induces a B to A transition in DNA (14, 18). CD spectra were recorded for the DNA 18-mer in 60, 65 and 70% TFE (v/v), conditions under which the oligonucleotide remains double stranded (Fig. 1b). The DNA 18-mer spectra exhibit increasing positive and negative ellipticity at 270 and 210 nm, respectively, with increasing TFE concentration. Comparison to the RNA 18-mer spectrum(Fig. 1a) reveals an apparent B to A transition. The DNA 9-mer exhibits a similar B to A transition between 60-70% TFE (data not shown). This range is comparable to TFE concentrations required to induce the transition in other DNA sequences (18). Other conditions were tested for the capacity to induce a B to A transition in the 9-mer. The B-form appearance of the CD spectrum is conserved in the presence of high salt concentrations (up to 2M NaCl) and in the buffer used for crystallization by Kennard and co-workers (12 mM Na cacodylate, 12 mM Na acetate, pH 6.5 (5)). Spermine was also added to

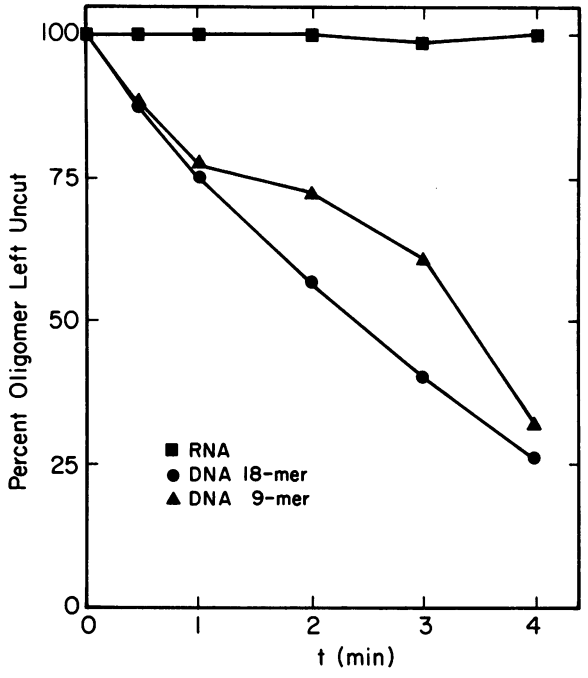

Figure 2
Cu-phenanthroline time course digestion of the RNA 18-mer r(GGAUGGGAGCUCC-CAUCC) (■), DNA 18-mer d(GGATGGGAGCTCCCATCC) (●), and the DNA 9-mer d(GGATGGGAG)·d(CTCCCATCC) (▲). The percent of uncut oligonucleotide is reported vs. the reaction time. Cu-phenanthroline is specific for B-form helices (see 16).

match more closely the conditions used in X-ray studies. No effect on the CD spectrum was observed for spermine concentrations up to 1.6 mM.

Chemical and Enzymatic Probes

The structures of the DNA and RNA 18-mers were probed with a variety of enzymes and the cleavage reagent 1,10-phenanthroline copper ion, which is reported to be specific for B-form helices (21). The DNA 9-mer and 18-mer were readily cleaved by 1,10-phenanthroline copper, whereas no activity was observed with the RNA oligomer (Fig. 2). As expected, the DNA was cleaved by DNase I and the restriction endonuclease Alu I, while double strand specific ribonuclease V1 efficiently cleaved the RNA (data not shown).

NMR

Assignments of the non-exchangeable aromatic proton resonances, as well as those of the H1', H2', H2" and methyl protons, were obtained from the NOESY spectrum, and cross-checked in the COSY spectrum, using standard sequential methods (22). The region of the NOESY spectrum corresponding to aromatic to H1' cross peaks is shown in Fig. 3, together with

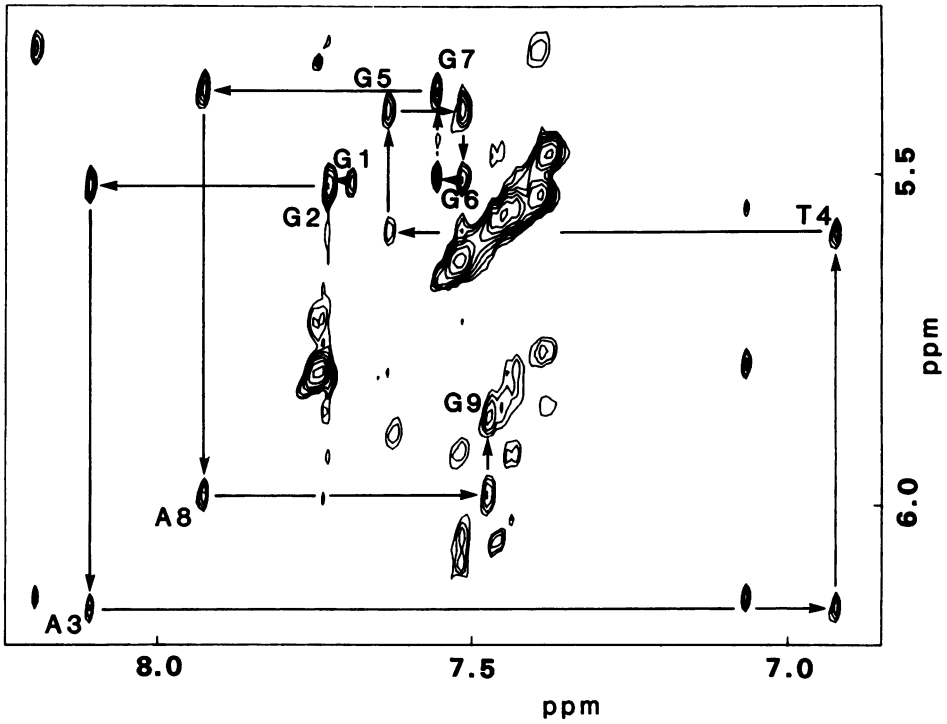

Figure 3
Sequential assignment of the 500 Mhz proton NMR spectrum using the aromatic to H1' connectivities observed in the NOESY spectrum at 250 ms mixing time. The aromatic to H1' connectivity pathway is shown for strand d(GGATGGGAG). Intranucleotide aromatic to H1' cross peaks are labeled. Assignments were confirmed using the connectivity path through the aromatic to H2', H2" region and the cross peaks between H1' and H2', H2" protons.

the connectivity pathway used for assignments for one of the strands. The H2' resonances were distinguished from the H2" resonances on the basis of the different shapes of their cross-peaks to H1' in the phase- sensitive COSY (see Fig. 4a). This distinction was confirmed by the relative intensity of the H1' to H2" vs. H1' to H2' cross peaks, the former always being stronger than the latter regardless of oligonucleotide conformation (23). For most residues, H2' was upfield from H2"; however, the chemical shifts of the H2' and H2" resonances were the same for the C18 residue, whereas H2" was downfield from H2' for the G9 residue. In addition, assignments for the H3' and H4', and a few of the H5' and H5" resonances were made using cross peaks to aromatic and sugar H1', H2' and H2" protons. Assignments are summarized in Table I.

One of the major differences between A- and B-form DNA is the conformation of the sugar, which can be conveniently described by means of the pseudorotation phase angle (24). In A-form DNA, the sugar pucker is 3'-endo, corresponding to a pseudorotation angle of 18°. In B-form

DNA the sugar pucker is usually found in the south family of conformers, frequently close to canonical 2'-endo (phase angle 162°). Magnitudes of the scalar couplings between nucleic acid sugar protons are very sensitive to the sugar conformation. Two-dimensional correlated spectroscopy (COSY) is a suitable technique for evaluating coupling constants, but direct measurements are frequently impossible because of peak overlap and limited digital resolution. However, measurements of individual coupling constants is not necessary (25). Required information can be extracted from the knowledge of multiplet widths and splitting patterns in COSY spectra. The percent of time the individual sugar moieties are found in one of two major conformers while undergoing rapid conformational equilibrium can also be derived. Some cross peaks from the region of the COSY spectrum corresponding to the H1'/H2' and H1'/H2" sugar protons are shown in Fig. 4a. The multiplet widths $\Sigma_{1'}$, $\Sigma_{2'}$, and $\Sigma_{2"}$ (defined in Fig. 4a) along with the coupling constants $J_{1'2'}$ and $J_{1'2"}$ (measured as shown in Fig. 4b) are reported in Table II for all but residue C18. It was not possible to measure the coupling constants for the C18 residue because H1'/H2' and H1'/H2" cross peaks are superimposed. The value of $\Sigma_{1'}$ is an excellent marker for the relative population of the south and north conformers. Large values of $\Sigma_{1'}$ (>14.5 hz, see Table II) are a conclusive indication that the fraction of S-type conformer is greater than ~80% for most residues (25).

Once the major conformer is determined, the different shapes of the COSY cross peaks and the multiplet widths distinguish unambiguously the H2' from the H2" resonances (Fig 4a, see also 25 and 26). The splitting patterns of the H1', H2', and H2" are also qualitatively consistent with a larger population of the south conformer. This conformational purity is further confirmed by comparing the experimental cross-peak shapes of Figure 4a with recent simulations of the cross-peak patterns for various families of sugar pucker (26). Approximate percent south conformer and pseudorotation phase angles (25) have been determined for each residue (Table I). Overall, with the exceptions of C17 and C10, multiplet widths and coupling constants are only consistent with a contribution less than 20% from the north (C3'-endo) conformer. For most residues, multiplet widths and coupling constants are consistent with an average pseudorotation phase angle between 140° and 180° and a relatively large amplitude of pucker (~40°). High conformational flexibility at the 3' end of pyrimidine rich sequences, as seen here at C17, has been previously reported (27). Generally larger values of $\Sigma_{1'}$ and $J_{1'2'}$ indicate that the purine rich strand has less conformational flexibility than the pyrimidine rich strand (Table II). This findings agree with previous work on sequences containing homopurine-homopyrimidine tracts (27), but the conformational purity observed for our molecule is not seen in $d(C_3G_3)$, which also contains a tract of three consecutive guanines (Wolk et al., 1987 personal communication).

Nuclear Overhauser enhancement spectroscopy (NOESY) yields detailed information on the local structure of nucleic acid fragments since the distance between protons can be estimated from the magnitudes of the cross peaks between resonances. Distances between aromatic and sugar H2' and H2" protons are very different in A- and B-form nucleic acids (12). Given the sugar pucker

from the above analysis, it is possible to estimate the glycosidic angle from the intranucleotide cross-peak intensities. For C2'-endo pucker and A-form glycosidic angle, the aromatic to H1' distance (~3.6 Å) is comparable to the aromatic to H2' distance and much shorter than the aromatic to H2" (~4.5 Å). Conversely, for B-form glycosidic angle, the aromatic to H2' (≤2.5 Å) and aromatic to H2" distances (~3.5 Å) become shorter than the corresponding aromatic to H1' distance (23).The region of the NOESY spectrum corresponding to aromatic to H2' and H2" cross peaks is shown in Fig. 5. In this region of the spectrum, intranucleotide NOE's are generally stronger than internucleotide NOE's as expected for B-form, as opposed to A-form DNA. Intranucleotide cross peaks between aromatic and H2' and H2" are stronger than corresponding aromatic to H1' cross peaks. This pattern is typical of B-DNA, and indicates that the glycosidic angles are near the value expected for B-DNA. In A-DNA, aromatic to H2', H2" cross-peaks are as intense as aromatic to H1' cross-peaks (23). Very weak NOE's were observed between aromatic and sugar H3', H4' protons (data not shown). The absence or weakness of intra-nucleotide aromatic to H3' cross peaks is another indication of B-form geometry, since these protons should be much closer in A-DNA (3-3.2 Å) than in B-DNA (4.5-5 Å) (23). Inter-nucleotide cross-peaks between aromatic and H2" protons are stronger than the corresponding

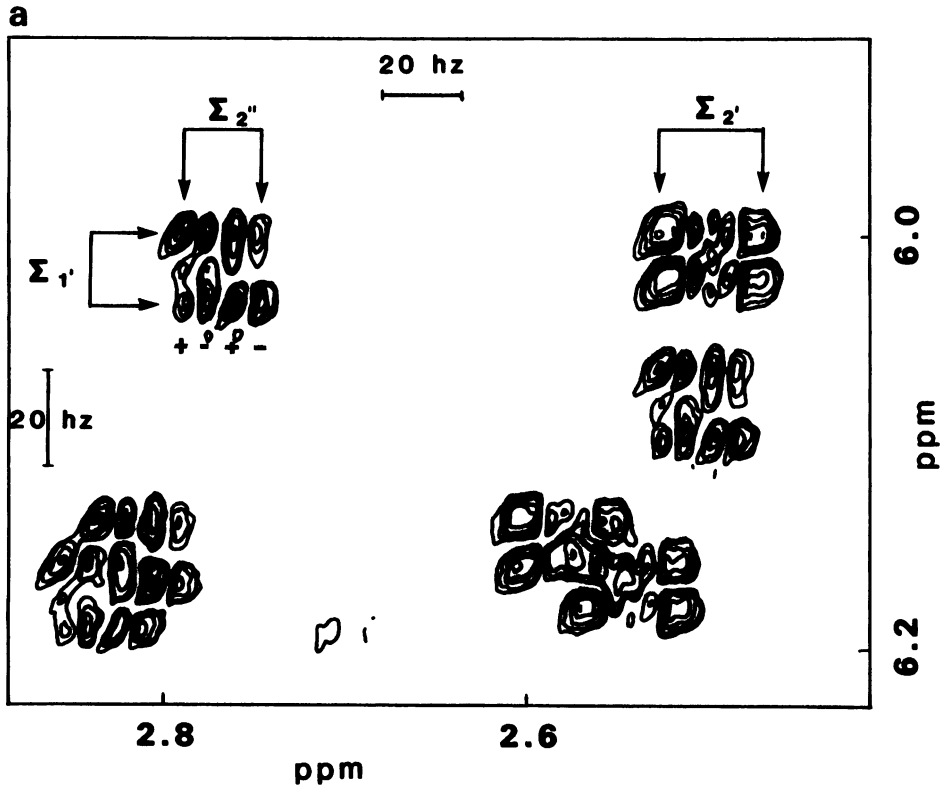

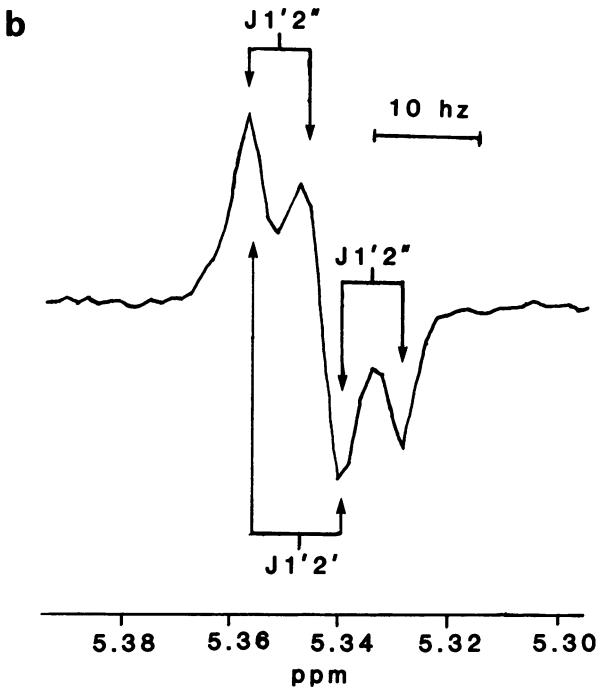

Figure 4

(a) Expanded view of part of the H1' to H2', H2" region of the COSY spectrum of d(GGATGGGAG)·d(CTCCCATCC). Starting from the upper left and moving clockwise the cross peaks correspond to A8 (H1' to H2"), A8 (H1' to H2'), T11 (H1' to H2"), A3, A15 (H1' to H2') (overlapped), and A3, A15 (H1' to H2") (overlapped). Note the difference in shape between cross peaks corresponding to H2' protons and those corresponding to H2" protons. Also indicated are the multiplet widths, $\Sigma_{1'}$, $\Sigma_{2'}$, and $\Sigma_{2''}$.

(b) Measurement of coupling constants $J_{1'2'}$ and $J_{1'2''}$. The 1D slice is through the H1', H2' COSY cross peak corresponding to residue C14.

aromatic to H2' cross-peaks and internucleotide NOE's between H2' and H1' protons were not observed. In A-DNA, aromatic protons are very close to neighboring H2' protons (~2.1 Å), whereas the internucleotide aromatic to H2" distance is longer (~4 Å). As a consequence, internucleotide aromatic to H2' cross peaks are expected to be much stronger than the corresponding aromatic to H2" in A-DNA.

DISCUSSION

Physical techniques and chemical and enzymatic probes were used as complementary tools for defining some features of the solution structure of the TFIIIA recognition fragment d(GGATGGGAG)·d(CTCCCATCC). This DNA duplex of 9 base pairs and an 18 base pair DNA duplex d(GGATGGGAGCTCCCATCC) containing a palindromic repeat of the 9-mer sequence have CD

Table I Chemical shifts of non-exchangeable protons in d(GGATGGGAG)·d(CTCCCATCC) relative to TSP.

$^{5'}$ G_1 G_2 A_3 T_4 G_5 G_6 G_7 A_8 G_9 $^{3'}$
$^{3'}$ C_{18} C_{17} T_{16} A_{15} C_{14} C_{13} C_{12} T_{11} C_{10} $^{5'}$

Proton 1'		2'	2"	3'	4'	6/8 (aromatic)	5/methyl
Residue							
G1	5.54	2.35	2.53	4.70	4.13	7.71	
G2	5.54	2.62	2.72	4.91	4.27	7.75	
A3	6.17	2.55	2.84	4.93	4.37	8.13	
T4	5.62	1.79	2.20	4.73	4.03	6.94	1.27
G5	5.43	2.47	2.58	4.85	4.20	7.64	
G6	5.53	2.42	2.57	4.86	4.23	7.53	
G7	5.40	2.42	2.57	4.86	4.21	7.57	
A8	6.01	2.50	2.77	4.90	4.31	7.95	
G9	5.90	2.26	2.15	4.50	4.05	7.50	
C10	5.78	2.16	2.48	4.55	4.00	7.79	5.87
T11	6.08	2.19	2.51	4.80	4.16	7.53	1.59
C12	5.89	2.11	2.39	4.74	4.10	7.48	5.59
C13	5.79	2.04	2.34	4.71	4.07	7.39	5.49
C14	5.34	2.05	2.31	4.71	4.01	7.41	5.55
A15	6.16	2.59	2.82	4.89	4.30	8.20	
T16	5.82	1.95	2.35	4.73	4.06	7.09	1.34
C17	5.96	2.11	2.36	4.70	4.04	7.46	5.59
C18	6.13	2.15	2.15	4.44	3.94	7.58	5.71

spectra characteristic of B-form structure. The spectra are very different from the A-form CD spectrum of an 18-mer RNA of identical sequence, suggesting B-form base stacking in the DNA. An apparent B to A conversion of the DNA oligonucleotides over 60-70 % TFE provides further evidence that in aqueous solution the fragment is in a conformation globally distinct from A-form. Likewise, enzymatic and chemical probe experiments confirm that this DNA sequence has properties distinct from those of A-RNA.

NMR data confirm that at the individual nucleotide level the DNA structure is B-form. The large values of the H1' multiplet widths ($\Sigma_{1'}$>14.5 hz), together with the shapes of the H1'-H2' and H1'-H2" cross-peaks, conclusively show that the sugar pucker is predominantly south for all but 2 residues. The values of coupling constants $J_{1'2'}$ and $J_{1'2"}$, together with the H2' and H2" multiplet widths, show that the sugar pucker is near 2'-endo as opposed to 3'-endo as expected

Table II Scalar coupling constants (J) and multiplet widths (Σ) for the sugar protons of d(GGATGGGAG)·d(CTCCCATCC), together with the evaluated structural parameters (percent south conformer and approximate pseudorotation phase angle). From left, entries to the column represent H1'-H2' and H1'-H2" coupling constant, H1', H2' and H2" multiplet width, percent south conformer and pseudorotation phase angle. The amplitude of pucker is ~40° for every residue. Uncertainty of the measured coupling constants and multiplet widths is ± 0.5 hz. Uncertainty in the pseudorotation phase angle is ±15°.

		$J_{1'2'}$	$J_{1'2''}$	$\Sigma_{1'}$	$\Sigma_{2'}$	$\Sigma_{2''}$	%S	Phase angle (°)
				Hz (±0.5)				
1	5'G	9.7	5.5	15.0	28.5	18.5	95±5	180
	G	10.6	4.9	15.4	/	19.8	100	160
	A	9.9	5.2	15.1	29.9	20.9	95±5	170
	T	9.6	5.1	14.7	30.5	21.5	90±10	150
5	G	10.9	4.7	15.3	30.0	18.8	100	150
	G	10.3	5.3	16.5	32.1	19.1	100	120
	G	10.7	4.9	15.6	28.3	20.8	100	170
	A	9.6	5.5	14.6	28.7	20.5	90±10	170
9	3'G	8.8	5.9	15.0	29.3	23.6	80±10	180
10	5'C	4.9	6.9	11.7	25.4	26.4	40±10	/
	T	9.8	4.9	15.3	30.0	20.7	95±5	170
	C	8.9	5.2	13.8	29.9	20.6	85±15	140
	C	9.0	5.6	14.6	29.4	20.9	90±10	170
	C	9.1	4.8	14.7	28.7	21.8	90±10	160
15	A	9.5	5.1	14.7	28.1	21.0	90±10	170
	T	8.8	5.8	14.7	30.3	20.9	80±10	120
	C	/	6.5	13.7	28.4	22.9	65±10	/
18	3'C	/	/	/	/	/	/	/

for A-DNA. In general, the pattern of NOE cross peaks at all mixing times (60 to 250 ms) are consistent with a B-form overall conformation, using interproton distances for standard A- and B-DNA derived from X-ray data as references (23). Intranucleotide cross peaks between aromatic and sugar protons prove that the glycosidic angle is characteristic of B-form. Internucleotide

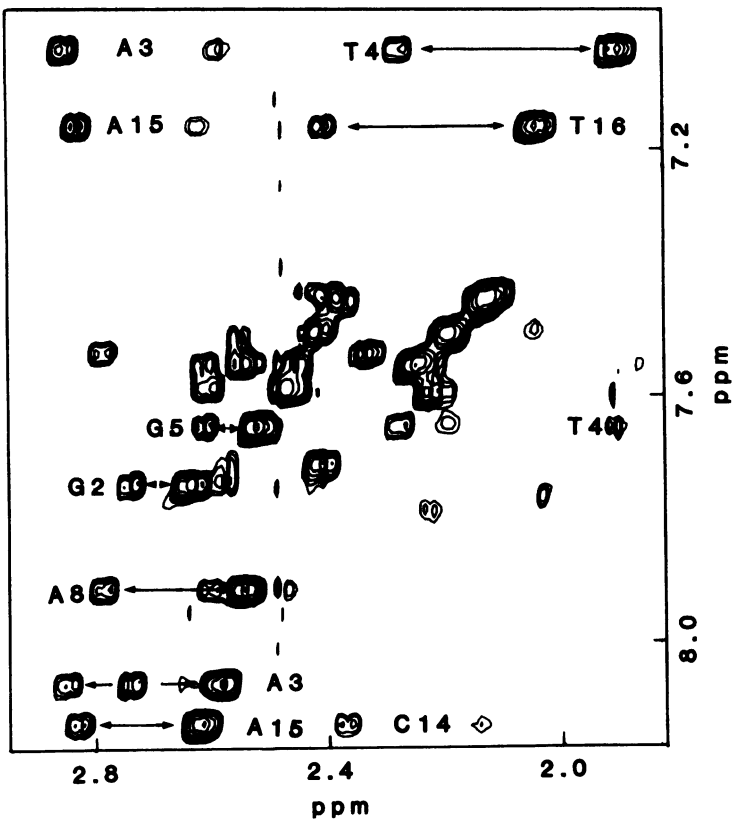

Figure 5
Region of the NOESY spectrum at 250 ms mixing time corresponding to aromatic to H2', H2" cross peaks. Four cross peaks are expected in this region for both A- and B-form DNA: the aromatic to its own H2', H2" protons and to the H2', H2" protons of its 5' neighbor. Cross peaks connected by arrows in the figure correspond to intranucleotide NOEs for the specified residues. For all labeled cross peaks the 2' cross peak is upfield (lower ppm) from the 2" cross peak. The fact that intranucleotide aromatic to 2" cross peaks are of comparable if not greater intensity than corresponding aromatic to H1' cross peaks (see Fig. 3) fixes the glycosidic angle to within the range expected for B-DNA.

aromatic to sugar NOE intensities are also consistent with B-form rather than with A-form geometry. This is most apparent from the relative intensities of the cross peaks between aromatic protons and neighboring H2', H2" protons. Superimposed on this general B-form pattern there are apparent local variations yet to be analyzed quantitatively. In summary, we find no evidence to support an A-form conformation for the DNA 9-mer in solution.

Since McCall et al. (5) determined that the same oligomer has an A-form structure in the crystal, several possibilities emerge. Crystal packing forces might induce a B-A transition for this TFIIIA fragment, as already suggested for other GC rich sequences (9, 10). Similarly, TFIIIA

binding may induce a B to A transition in the gene, as proposed on the basis of unwinding data (28). However, addition of TFIIIA protein to a solution containing the full 54 base pair binding site induced no dramatic change in the high wavelength (270 nm) CD band (11). Furthermore, we have found that the TFE concentrations required to convert the 9-mer and 18-mer to A-form DNA are similar to those necessary for other DNA sequences. Therefore, this fragment of the 5S RNA gene does not appear significantly more labile toward A-form than random sequence DNA.

Local variations in the conformation of d(GGATGGGAG)·d(CTCCCATCC) from typical B-form may explain the enzymatic digestion data of Klug and coworkers and, perhaps, the structural features observed in the crystal. Recent combined NMR and molecular mechanics studies indicate that, within an overall B structure, values of base pair roll and slide may be more similar to A-form DNA between certain residues (13). Local A-form structural features may influence enzymatic digestion experiments (2, 3) and play a role in the specific recognition of the gene by TFIIIA. Variations of the structure within a general B-DNA geometry are suggested by variations in the relative intensities of internucleotide cross peaks (Fig. 3). We are exploring the possible existence of local structural variations by obtaining a high-resolution solution structure for the TFIIIA fragment using distance geometry and other NMR-based methods (29). We are encouraged by the conformational purity revealed by the data in Table I since conformational equilibria tend to hinder methods for obtaining structures based on NMR.

ACKNOWLEDGMENTS

This investigation was sponsored by USPH-NIH grant GM10840 and DOE grant DE-FG03-86ER60406. The authors were supported by EHS Training Grants 5 T32 ES07075-09 (F. A.) and ES07075-10 (G. T. W.), and by Foundation A. Della Riccia (G. V.). We are grateful to David Koh for aid in oligonucleotide synthesis and to Steven Wolk and Dr. Lambertus Rinkel for helpul discussion.

REFERENCES

1. Brown, D. D. (1980) The Harvey Lectures **76**, 27-44.
2. Fairall, L., Rhodes, D., and Klug, A. (1986) J. Mol Biol. **192**, 577-591.
3. Rhodes, D., and Klug, A. (1986) Cell **46**, 123-132.
4. Hanas, J. S., Bogenhagen, D. F., and Wu, C.-W. (1984) Nucleic Acids Res. **12**, 2745-2758.
5. McCall, M., Brown, T., Hunter, W. N., and Kennard, O. (1986) Nature **322**, 661-664.
6. Sakonju, S., and Brown, D. D. (1982) Cell **31**, 395-405.
7. McCall, M., Brown, T., and Kennard, O. (1985) J. Mol. Biol. **183**, 385-396.
8. Wang, A. H. J., Fujii, S., van Boom, J. H., and Rich, A. (1982) Nature **299**, 601-604.
9. Benevides, J. M., Wang, A. H. J., Rich, A., Kyogoku, Y., van der Marel, G. A., van Boom, J., H., and Thomas, G. J., Jr. (1986) Biochemistry **25**, 41-50.
10. Rinkel, L. J., Sanderson, M. R., van der Marel, G. A., van Boom, J. H., and Altona, C. (1986) Eur. J. Biochem. **159**, 85-93.
11. Gottesfeld, J. M., Blanco, J., Tennant, L. L. (1987) Nature **329**, 460-462.
12. Haasnoot, C. A. G., Westerink, G. A., van der Marel, G. A., and van Boom, J. H. (1983) J. Biomol. Struc. Dynamics **2**, 345-360.
13. Nilges, M., Clore, G. M., Gronenborn, A. M., Brunger, A. T., Karplus, M., and Nilsson,

L. (1987) Biochem. **26**, 3718-3733.
14. Riazance, J. H., Baase, W. A., Johnson, W. C., Jr. , Hall, K., Cruz, P., and Tinoco, I., Jr. (1985) Nucleic Acids Res. **13**, 4983-4989.
15. Milligan, J. F., Groebe, D. R., Witherell, G. W., and Uhlenbeck, O. C. Nucleic Acids Res., in press.
16. Kuwabara, M., Yoon, C., Goyne, T., Thederahn, T. and Sigman, D. S., (1986) Biochemistry **25**, 2401-2408.
17. Ernst, R. R., Bodenhausen, G., and Wokaun, A., (1987) Principles of Nuclear Magnetic Resonance in One and Two Dimensions (Clarendon Press-Oxford).
18. Minchenkova, L. E., Scholkina, A. K., Chernov, B. K., and Ivanov, V. I. (1986) J. Biomol. Struc. Dynamics **4**, 463-476.
19. Gray, D. M., Liu, J-J., Ratliff, R. L., and Allen, F. S. (1981) Biopolymers **20**, 1337-1382.
20. Allen, F. S., Gray, D. M., and Ratliff, R. L. (1984) Biopolymers **23**, 2639-2659.
21. Marshall, L. E., Graham, D. R., Reich, K. A., and Sigman, D. S. (1981) Biochem. **20**, 244-250.
22. Hare, D. R., Wemmer, D. E., Chou, S. H., Drobny, G., and Reid, B. R. (1983) J. Mol. Biol. **171**, 319-336.
23. Wuthrich, K. (1986) NMR of Proteins and Nucleic Acids (John Wiley and Sons, Inc. New York).
24. Altona, C., and Sundaralingam, M. (1973) J. Am. Chem. Soc. **95**, 2333-2344.
25. Rinkel, L. J., and Altona, C. (1987) J. Biomol. Struc. Dynamics **4**, 621-649.
26. Widmer, H. D., Wüthrich, K. (1987) J. Mag. Res. **74**, 316-336.
27. Rinkel, L. J., van der Marel, G. A., van Boom, J. H., and Altona, C. (1987) Eur. J. Biochem. **166**, 87-101.
28. Reynolds, W. F., and Gottesfeld, J. M. (1983) Biochem. **80**, 1862-1866.
29. Patel, D. J., Shapiro, L., and Hare, D. (1987) Ann. Rev. Biophys. Biophys. Chem. **16**, 423-453.